HHS Public Access

Author manuscript

Nat Med. Author manuscript; available in PMC 2014 September 01.

Published in final edited form as:

Nat Med. 2014 March ; 20(3): 301–306. doi:10.1038/nm.3460.

Non-invasive Imaging of *Staphylococcus aureus* Infections with a Nuclease-Activated Probe

Frank J. Hernandez[1], **Lingyan Huang**[2], **Michael E. Olson**[3], **Kristy M. Powers**[2], **Luiza I. Hernandez**[1], **David K. Meyerholz**[4], **Daniel R. Thedens**[5], **Mark A. Behlke**[2], **Alexander R. Horswill**[3], and **James O. McNamara II**[1,6]

[1]Department of Internal Medicine, Roy J. and Lucille A. Carver College of Medicine, University of Iowa, Iowa City, IA 52242, USA

[2]Integrated DNA Technologies, Inc. (IDT), Coralville, IA 52241, USA

[3]Department of Microbiology, Roy J. and Lucille A. Carver College of Medicine, University of Iowa, Iowa City, IA, USA

[4]Department of Pathology, Roy J. and Lucille A. Carver College of Medicine, University of Iowa, Iowa City, IA, USA

[5]Department of Radiology, Roy J. and Lucille A. Carver College of Medicine, University of Iowa, Iowa City, IA, USA

Abstract

Technologies that enable the rapid detection and localization of bacterial infections in living animals could address an unmet need for infectious disease diagnostics. We describe a molecular imaging approach for the specific, non-invasive detection of *S. aureus* based on the activity of its secreted nuclease, micrococcal nuclease (MN). Several short, synthetic oligonucleotides, rendered resistant to mammalian serum nucleases by various chemical modifications, flanked with a fluorophore and quencher, were activated upon degradation by recombinant MN and in *S. aureus* culture supernatants. A probe consisting of a pair of deoxythymidines flanked by several 2′-*O*-methyl-modified nucleotides was activated in culture supernatants of *S. aureus* but not in culture supernatants of several other pathogenic bacteria. Systemic administration of this probe to mice

[6]To whom correspondence should be addressed: James-McNamara@uiowa.edu.

Author contributions F.J.H. developed the experimental methodology, designed experiments, carried out experiments and analyzed data. L.H., M.E.O. and K.M.P. generated novel reagents and provided critical technical input. M.E.O. also measured the CFUs of bacterial cultures. L.I.H. measured blood counts of mice. D.K.M. carried out the histological staining and data analysis. D.R.T. carried out the magnetic resonance imaging and analysis. M.A.B. provided critical input for probe design and generation, oversaw probe generation and contributed to the conceptual development of the project. J.O.M., A.R.H. and F.J.H. conceived and developed the underlying concepts of the project. A.R.H. oversaw the generation of genetically modified bacteria and the preparation of bacterial cultures. J.O.M. designed experiments, analyzed data, coordinated the various aspects of the project and wrote the manuscript with help from all of the authors.

All animal experiments were approved by the University of Iowa Institutional Animal Care and Use Committee (IACUC).

Competing Financial Interests The authors declare competing financial interests. F.J.H., L.H., M.A.B., A.R.H., and J.O.M. are inventors on a patent application that covers the technology described in this study. M.A.B., L.H., and K.P. are employed by Integrated DNA Technologies, Inc., (IDT) which offers oligonucleotides for sale similar to some of the compounds described in the manuscript. IDT is however not a publicly traded company and these authors do not personally own any shares or equity in IDT.

bearing bioluminescent *S. aureus* muscle infections resulted in probe activation at the infection sites in an MN-dependent manner. This novel bacterial imaging approach has potential clinical applicability for *S. aureus* and several other medically significant pathogens.

Introduction

Diagnosis of focal bacterial infections, such as osteomyelitis, septic arthritis and pyomyositis, initially entails the evaluation of several non-specific symptoms, including pain, swelling and fever.[1–3] Definitive evidence of infection and identification of the causative bacterial species is only possible with tissue biopsy and culture. While focal bacterial infections can be life-threatening situations in which time is of-the-essence, such diagnostic procedures typically consume many hours to days. Moreover, current diagnostic approaches are prone to false-negatives.[4] Rapid, sensitive and non-invasive molecular imaging assays for bacterial infections could thus address an unmet need for infectious disease diagnostics.

Preclinical development of molecular imaging approaches for bacterial infections offers hope for the future availability of such technologies.[5–11] While promising, none of these approaches provides a platform for the development of species-selective imaging probes for multiple bacterial species. Bacterial imaging probes that provide species-specific information are desirable because they could facilitate the rapid administration of appropriate therapy (e.g., antibiotic selection) in clinical settings. Nucleases are one category of proteins that could be used to specifically identify a variety of bacterial species due to their widespread expression and diversity.[12] As degrading enzymes, nucleases can be detected with activatable probes.[13] Activatable probes only exhibit signal (usually fluorescence) upon encountering their target molecule, which greatly increases the sensitivity of target detection, and thus provides an important advantage over non-activatable probes.[14] We recently reported that several, as yet unidentified nucleases produced by a species of mycoplasma (*Mycoplasma fermentans*) can efficiently digest chemically modified oligonucleotides that are resistant to degradation by mammalian nucleases.[15] This finding suggested the use of chemically modified oligonucleotides as the basis of activatable probes for the detection of *Mycoplasma fermentans*.

We began the present study by asking whether bacterial pathogens that are responsible for substantial morbidity and mortality might also express nucleases capable of degrading chemically modified oligonucleotides. Such nucleases could potentially be used as the probe-activating component of a pathogenic bacterial imaging approach. We focused our efforts on *S. aureus*, the most common cause of many types of focal infections in humans.[1–3] *S. aureus* secretes a nuclease known as micrococcal nuclease (MN), a very well-studied enzyme that is among the first proteins extensively investigated with structure and folding studies.[16–18] MN exhibits robust DNase and RNase activities, is active on both single- and double-stranded DNA substrates, and its nuclease activity has been used to classify bacterial isolates for decades.[17, 19]

Here we report the non-invasive detection of *S. aureus* infections with a quenched fluorescent oligonucleotide probe that was tailored to be specifically activated by MN. The

probe is expected to be both non-toxic and inexpensive and it enabled infection localization in less than an hour when administered at low doses. These elements could facilitate the translation of this infection imaging approach into clinical practice.

Results

We sought a short oligonucleotide substrate that is both sensitive to MN and resistant to serum nucleases. Such an oligo could form the basis of a quenched fluorescent imaging probe that is specifically activated (fluorescence is unquenched) upon digestion by MN.[13] Because the susceptibility of chemically modified oligonucleotide substrates to MN digestion is poorly understood, we tested the ability of MN to degrade oligonucleotide substrates with chemical modifications that are known to promote resistance to degradation by mammalian serum nucleases.[20] To facilitate the subsequent development of imaging probes, we tested the various oligo compositions in a quenched fluorescent probe format: short (10–12mer) oligos flanked with a 5′-fluorophore (fluorescein amidite (FAM)) and 3′-quenchers (ZEN and Iowa Black RQ).[13, 15]

One such probe, made with an oligo composed exclusively of locked nucleic acid–modified nucleotides, was not digested by MN (FJH, unpublished observations), while oligos composed exclusively of 2′-fluoro- or 2′-*O*-methyl-modified nucleotides were relatively weak substrates (not shown).[20, 21] Next, we compared the MN- and serum nuclease-susceptibility of RNA oligos composed of 2′-fluoro- or 2′-*O*-methyl-modified pyrimidines and unmodified purines, with a DNA oligo, as DNA is the preferred substrate for MN among unmodified nucleic acids (see Table 1 for probe sequences and modifications).[17] A 1 U μl^{-1} MN concentration yielded complete or near-complete digestion of these oligos after short incubations and was thus used as a normalization control for the assays. More dilute MN (0.1 U μl^{-1}) provided an intermediate degree of digestion after 15 or 60 minutes, thus enabling assessment of the relative degree of digestion of the substrates. As shown (in Fig. 1a), the DNA probe was digested by MN more efficiently than either the 2′-fluoro- or 2′-*O*-methyl- modified pyrimidine RNA oligos, but was, as expected, also substantially digested in serum. In contrast, the 2′-fluoro- and 2′-*O*-methyl- modified pyrimidine RNA oligos were more stable in serum, but less efficiently digested by MN. A second generation probe, composed of a pair of deoxythymidines flanked by several 2′-*O*-methyl modified nucleotides, was designed to maximize sensitivity to MN, which is known to efficiently digest oligos with deoxythymidine nucleotides, while also resisting serum nuclease degradation.[22] This “TT probe” was substantially more sensitive to MN digestion than the other chemically modified oligos tested, and also exhibited robust serum stability (Fig. 1a). Probes in which AT or AA were substituted for the central TT exhibited reduced sensitivity for MN digestion and were not pursued with further experiments (see Supplementary Fig. 1). Measurement of TT probe activation by MN (0.05 U μl^{-1}) as a function of time revealed rapid activation kinetics, with an activation half-time of 7.7 minutes (see Supplementary Fig. 2). The TT probe exhibited comparable activation by MN in the context of mouse or human serum and buffer (PBS), suggesting its *in vivo* utility (see Supplementary Fig. 3).

To evaluate the activation of these probes in the context of the complex mixture of *S. aureus*-secreted factors, the probes were incubated with culture supernatants of the Newman

and UAMS-1 strains of *S. aureus* (Fig. 1b). The TT probe was completely digested after a 60-minute incubation in either supernatant (Fig. 1b). This was not unexpected because we previously measured extracellular MN levels of 0.45–0.6 U μl^{-1} in cultures of these strains.[23] The digestion observed here was primarily mediated by MN as incubation of the TT probe in supernatants of MN-negative versions of each strain yielded minimal probe activation (Fig. 1b).[23, 24] In summary, among the serum-nuclease-resistant oligos tested, the TT probe clearly exhibited the greatest sensitivity to digestion by MN, both in purified form and in culture supernatants.

The utility of visible light fluorophores, such as fluorescein (excitation/emission (ex/em), 494/521 nm), for *in vivo* imaging is severely limited by tissue autofluorescence and scattering of visible light.[25] In contrast, tissue penetration of light with substantially longer wavelengths, especially within the near-infrared (NIR) range, is much greater and tissue autofluorescence is minimal.[25] Indeed, fluorescence imaging with NIR light is estimated to be feasible at tissue depths of 7–14 cm.[25] To prepare an MN-detecting imaging probe based on the TT probe that would be more suitable for *in vivo* imaging, we substituted Cy5.5 (ex/em: 685/706 nm), a fluorophore with emission in the NIR range, for the FAM moiety used in the initial TT probe version. The fluorescence of this intact probe was weak, but after digestion with MN, its fluorescence was comparable to that of a control probe, synthesized without fluorescence quenchers (Fig. 2a).

Next, we sought to determine whether this probe could enable the detection of a focal *S. aureus* infection in mice. To provide an independent measure of bacteria location and burden in infected animals, we incorporated the *lux* operon of *Photorhabdus luminescens* into wildtype *S. aureus* strain Newman and an MN-negative mutant.[26–28] Mice with unilateral thigh muscle infections (pyomyositis) of these modified bacteria exhibited luminescence that co-localized with clinical swelling and gross lesions (Fig. 2d,e & Supplementary Fig. 4). Magnetic resonance imaging of infected mice provided an additional measure of the lesions *in vivo* (Supplementary Fig. 5). Tail vein administration of 3 nanomoles (~1 mg kg^{-1}) of Cy5.5-labeled TT probe (probe was administered 48 hours after bacterial inoculation) yielded fluorescence at the infection sites that was evident as early as 15 minutes after injection (Fig. 2d). The subsequent accumulation of activated probe over time is possibly a result of the hydrophobic nature of the Cy5.5 dye, which may retard its clearance. In contrast to the probe activation seen in infected animals, injection of the Cy5.5-labeled TT probe into uninfected mice (Fig. 2b) did not yield lateralized probe activation. Administration of the unquenched TT probe into uninfected animals resulted in a globally high fluorescence that only began to decline 1–2 hours after injection (Fig. 2c and Supplementary Fig. 6). Finally, the probe activation seen at wildtype *S. aureus* infection sites was primarily due to the activity of MN as substantially less TT probe activation was seen at MN-negative *S. aureus* infection sites (Fig. 2e). Comparable luminescence levels were found in the wildtype and MN-negative *S. aureus* infections, indicating comparable bacterial loads in these experimental groups (Supplementary Fig. 7). The weak TT probe activation observed in the MN-negative infections likely results from a distinct *S. aureus* nuclease that has previously been described.[29] Weak TT probe activation observed upon incubation with MN-negative *S. aureus* cell suspensions (data not shown) is consistent with

this conclusion. There were no overt differences in the extent of bacterial colonization, necrosis or inflammation between the wildtype and MN-negative infections in histologic sections, or in levels of circulating neutrophils in mice bearing these infections (Supplementary Fig. 8,9). Thus, the probe activation seen in the wildtype *S. aureus*-infected animals does not appear to be related to the inflammatory response to the infections. Quantification of probe fluorescence levels at the infection sites and in the uninfected leg of TT probe-injected mice yielded an approximately 4-fold target-to-background ratio at 45 minutes post-probe injection (Supplementary Fig. 10).

While these results indicate that MN activates the TT probe at *S. aureus* infection sites *in vivo*, we observed that much of the probe fluorescence extended beyond the boundary of the bioluminescence signal. A simple and plausible explanation is that the intravenously administered probe may have limited access to the infection site in the setting of our pyomyositis infection model. Indeed, when bacterial infections progress to the stage of tissue necrosis, liquefaction, or abscess formation, penetration of intravenously administered agents (including antibiotics) is limited and access becomes problematic.[30] To explore this possibility, we injected the unquenched TT probe into *S. aureus*–infected mice. The mice were subsequently sacrificed and dissected to provide a clearer picture of the infection sites. As shown (in Fig. 2f), the unquenched probe appears to have very limited access to the infection site. Activation of the TT probe adjacent to the infection site was also observed after sacrifice and dissection (Fig. 2g). Moreover, histological examination of *S. aureus*–infected mouse thigh muscles (Supplementary Fig. 11) revealed lesions with substantial necrosis, an observation consistent with the notion that the infection sites have reduced blood perfusion, and consequently reduced probe access. These results suggest that the probe activation seen in infected animals (Fig. 2d,g) may have resulted from the probe encountering MN that had leaked out of the primary infection site. The rate that MN (a ~17 kDa protein) would need to penetrate the muscle tissue to account for the probe activation observed (~4 mm/48 hours = 0.08 mm hr^{-1}) is well within the limits found by others who have studied macromolecular penetration of muscle tissue (0.39–0.6 mm hr^{-1} for a 20 kDa dextran).[31] In summary, the TT probe detected the presence of *S. aureus*, despite having only limited access to the region where the bacteria, and presumably MN, were most concentrated.

The clinical diagnostic value of assays that non-invasively detect bacterial infections such as pyomyositis, septic arthritis, etc., will depend, in part, on their ability to simultaneously identify the type of bacteria that is present. We thus sought to determine whether the TT probe, or any of the others we have tested, might also be activated by nucleases produced by other bacterial pathogens that cause some of the same types of infections as *S. aureus*. Of the culture supernatants of seven such bacterial species tested (see Supplementary Table 2 for CFU ml^{-1} values), none substantially digested the TT probe, while *Staphylococcus lugdunensis* and *Streptococcus agalactiae* (Group B Streptococcus) supernatants both digested the probes that included 2′-fluoro modified nucleotides (Fig. 3a). The lack of activation of the DNA probe by culture supernatants of bacteria which are known to secrete DNases (e.g., *S. agalactiae*), possibly reflects an incompatibility of the particular sequence used in this probe with the secreted DNases. Of the bacterial cell suspensions of the cultures,

only the *Staphylococcus lugdunensis* (an emerging pathogen of the same genus as *S. aureus*) produced any appreciable digestion of the TT probe (~25%) in a one-hour incubation (Fig. 3b). Bacterial cell suspensions of *Streptococcus agalactiae* and *Streptococcus pneumoniae* both digested the probes that included 2′-fluoro modified nucleotides (Fig. 3b), possibly resulting from the activity of surface-localized nucleases. Together, these results demonstrate a high degree of nuclease specificity for the TT probe.

Discussion

The imaging tools that are currently available for diagnosing bacterial infections cannot directly detect bacteria or material derived from them; they are used to measure downstream consequences of infections, such as tissue destruction or inflammatory responses. Such assays provide no direct evidence of either the type or presence of bacteria at sites of potential infections. As a result of these limitations, physicians currently depend heavily on a variety of non-specific criteria together with biopsy and culture (which is time-consuming) to diagnose infections. In this proof-of-concept study, we developed an activatable probe that enables the non-invasive imaging of *S. aureus* infections in mice in less than an hour. To the best of our knowledge, the present study is the first to demonstrate the non-invasive imaging of a disease condition in animals with a nuclease-activated probe.

Our exploration of the substrate specificity of MN provided a framework for the design of a probe that would be efficiently activated by MN, without being susceptible to serum nucleases. The incorporation of unmodified deoxythymidines into the TT probe was intended to make it highly sensitive to MN digestion, and *in vitro* probe activation assays with purified MN indicate that MN does, in fact, efficiently activate the probe. Culture supernatants of two common strains of *S. aureus* also activate the probe. The activation of the TT probe by *S. aureus* (supernatants or in infected animals) can be attributed to MN activity because minimal probe activation was seen in experiments with an *S. aureus* mutant that does not express MN. Importantly, the TT probe is resistant to degradation by mouse and human serum nucleases, likely the result of the 2′-*O*-methyl modified nucleotides that flank the central deoxythymidines, as this modification is known to provide a high degree of resistance to serum nucleases. The nucleases present in the culture supernatants of the panel of additional pathogenic bacterial species failed to digest any of the oligos with 2′-*O*-methyl modified nucleotides. The inclusion of the flanking 2′-*O*-methyl modified nucleotides in the TT probe may thus be responsible for its specificity for MN versus these other bacterial nucleases. In any case, the fact that this probe exhibits specificity for MN suggests that the imaging approach described here has the potential not only to localize bacterial infections, but also to indicate the type of bacteria that may be present.

Several preclinical bacterial imaging approaches can detect bacteria non-specifically.[6–8, 10, 11] Our approach and the prothrombin-based approach of Panizzi et al., provide a means of specifically detecting *S. aureus*.[9] While non-specific bacterial detection has the advantage of detecting a wide variety of infections, species-specific detection can potentially guide physicians in antibiotic selection at an early stage in the diagnostic process, and thus provides complementary, and highly valuable information. In contrast to the prothrombin-based approach, the nuclease-activated approach provides a blue-print for the

species-specific detection of a variety of medically significant bacterial pathogens. The present study therefore represents a proof-of-concept study, which may lead to a new category of species-specific, activatable imaging probes for bacterial infections. The broad diversity of nuclease structures and enzymatic mechanisms supports the notion that specific probes can be engineered for many additional target nucleases.[12] Indeed, the distinct substrate specificities of the other (non-*S. aureus*) bacterial nucleases tested and the fact that some of these can digest oligos that are resistant to serum nucleases suggests the broader applicability of the approach. While this approach is only applicable to pathogens that produce targetable nucleases, there are, nonetheless, several prominent pathogens besides *S. aureus* that are known to produce robust nuclease activity.[32–34] The wide variety of existing synthetic nucleotide modifications is also likely to facilitate the engineering of additional specific probes.[20]

The bacterial detection approach we describe here seems well-suited for clinical translation. The probes are expected to be non-toxic because the oligonucleotide portion is composed only of naturally occurring, modified (2′-*O*-methyl) and DNA nucleotides. A recent pre-clinical toxicity study of IRDye 800CW, an NIR fluorophore that would be an attractive alternative to Cy5.5 for clinical translation of the approach (it is excited and emits at longer wavelengths which yield better tissue penetration) found low toxicity in rats.[35] TT probe activation was detected at infection sites after administration of low doses (~1 mg/kg), further increasing the likelihood that toxic effects can be avoided. Current nucleic acid synthesis and conjugation technologies are sufficiently advanced to make the large-scale GMP synthesis of such probes both feasible and economical. While deep-tissue infections (e.g., kidney abscesses) are beyond the reach of current non-invasive optical imaging approaches, there remains a wide variety of bacterial infections that is shallow enough to be detectable with NIR fluorescence imaging (e.g., many joint and bone infections). Ongoing efforts by several groups to translate NIR imaging approaches to the clinic may make NIR clinical imaging instrumentation commonplace in clinical settings in the near future, thus providing an infrastructure for the accommodation of NIR-based bacterial imaging diagnostic approaches.[36–39] For these reasons and the fact that this approach would address an important unmet clinical need, we anticipate its clinical translation in the coming years.

Online Methods

Oligonucleotide probe synthesis and purification

Oligonucleotide probes were synthesized and purified at Integrated DNA Technologies (IDT). Briefly, all the FAM-labeled probes were synthesized using standard solid phase phosphoramidite chemistry, followed by high performance liquid chromatography (HPLC) purification. For the Cy5.5-labeled probes, the sequences were first synthesized with ZEN and Iowa Black quenchers or inverted dT on the 3′-ends and amine on the 5′-ends using the standard solid phase phosphoramidite chemistry, and purified with HPLC. We set these purified sequences to react with Cy5.5 NHS ester (GE Healthcare) (to chemically conjugate the Cy5.5 label to the sequences) and then isolated the Cy5.5-labeled probes with a second HPLC purification. We confirmed all probe identities with electron spray ionization mass spectrometry (ESI-MS) using an Oligo HTCS system (Novatia LLC). The measured

molecular weights are within 1.5 Daltons of the expected molecular weights. The purity of the probes, as assessed with HPLC analysis, is typically greater than 90%. Quantitation of the probes was achieved by calculating from their UV absorption data and their nearest-neighbor-model-based extinction coefficients at 260 nm. Extinction coefficients of 2′-*O*-methyl-nucleotides and 2′-fluoro-nucleotides are assumed to be the same as that of RNA.

Fluorescence plate-reader nuclease assays

Fluorescence plate-reader assays were carried out as described.[15] Briefly, for each reaction, we combined 1 μl of a stock solution of each probe (50 μM concentration) with 9 μl of each sample (buffer, buffer plus recombinant nuclease, serum, culture supernatant, culture broth or washed bacteria) and incubated at 37 °C for the time periods indicated in the figures. We then added 290 μl of PBS supplemented with 10 mM EDTA and 10 mM EGTA to each and then loaded 95 μl of each diluted reaction per well into a 96-well plate (96F non-treated black microwell plate (NUNC)). We measured fluorescence levels with an Analyst HT fluorescence plate reader (LJL Biosystems). We measured background fluorescence levels of probes incubated in buffer or broth, and autofluorescence levels of the various preparations and subtracted them from the probe-activation reaction values as described in the figure legends. We obtained purified MN from Worthington Biochemical Corporation, Dulbecco's phosphate-buffered saline (DPBS), containing physiological levels of calcium and magnesium, from Invitrogen, human serum from Sigma-Aldrich and mouse serum (C57BL6) from Valley Biomedical Inc.

In vitro evaluation of the Cy5.5-TT probe

We incubated 10, 40, 160 or 640 picomoles of the Cy5.5-TT probe in 100 μl DPBS or DPBS + 1 U μl^{-1} MN at 37 °C for 1 hour. We measured fluorescence in 96-well plates in a Xenogen IVIS 200 imaging system. Controls include buffer only (DPBS) and equivalent amounts of the unquenched TT probe.

Bacterial cultures and growth conditions

We maintained bacteria in tryptic soy broth (TSB), Luria Bertani (LB) or Todd Hewitt + yeast (THY) broth as defined (see Supplementary Table 1) for each strain. To prepare cultures for assays, we sub-cultured overnight cultures 1:500 into 5 ml fresh broth and grew for 24 hr at 37 °C with shaking at 200 rpm. The only exceptions were *Streptococcus pneumoniae* and *Streptococcus agalactiae* (Group B Streptococcus), which were grown under static conditions in a 37 °C incubator supplemented with 5.0% CO_2. To prepare spent media for nuclease assays, we centrifuged 1 ml of each culture at 6,000 × g for 10 min and saved the supernatant. To prepare bacteria suspensions for nuclease assays, we washed pelleted bacteria with 1 ml DPBS and re-suspended in 100 μl of DPBS.

Genetic manipulation of *S. aureus*

Bacteriophage 11 was used to transduce the *P. luminescens luxABCDE* genes from AH1362 into strains Newman and Newman *nuc*::LtrB as previously described.[40] We selected transductants carrying the *lux* genes on tryptic soy agar (TSA) with kanamycin (Kan)

supplemented at 50 μg ml^{-1}. We confirmed bioluminescence production (*lux*+) in the resulting strains using a Tecan Infinite M200 plate-reader (see Supplementary Table 1).

S. aureus pyomyositis model

We prepared *S. aureus* cultures for injection into mice as follows. First, we inoculated 5 ml of TSB supplemented with Kan (50 μg ml^{-1}) with frozen stocks of MN-expressing or MN-negative *lux*+ *S. aureus* of the strain Newman genetic background (Supplementary Table 1). We grew the cultures overnight at 37 °C with shaking at 200 rpm, and then sub-cultured each strain 1:100 into 5 ml of fresh media and grew for another 12 hr at 37 °C with shaking. We washed the bacteria once with PBS and then re-suspended in PBS to an approximate cell density of ~2×10^8 CFU ml^{-1} for injection into mice. We serially diluted the bacteria, plated on TSA, and incubated at 37 °C to determine bacterial concentration.

For animal infections, we injected 50 μl of 2×10^8 CFU ml^{-1} (1×10^4 CFU total) intramuscularly (thigh muscle) in 6–8 week old C57BL6 female mice under isoflurane anesthesia. Mice were shaved prior to injections. We evaluated injection sites with bioluminescence imaging immediately thereafter. Mice were imaged or sacrificed for imaging, blood harvest or histology 48 hours after injections.

In vivo evaluation of nuclease-activated probes

We carried out luminescence and epifluorescence imaging with a Xenogen IVIS 200 imaging system (Caliper). First, we anesthetized mice with 2% isoflurane gas anesthesia and placed them on the imaging platform in the optical system for dorsal imaging. We recorded luminescence images with a 1 minute exposure time and an open emission filter. We recorded epifluorescence images with a 1 second exposure time and excitation and emission filters appropriate for the Cy5.5 dye. To avoid saturation, we reduced the exposure time for the acquisition of epifluorescence images of the mice injected with the unquenched TT probe to 0.5 seconds. We acquired bioluminescence and fluorescence images prior to probe injections and then additional fluorescence images were acquired following tail-vein injections (time points are indicated in figures) of the probes. For probe administration, we injected 3 nanomoles of each probe diluted in 120 μl PBS via tail vein. We used IVIS 4.2 software to perform acquisition, image processing (including soft binning and smoothing) and analysis and preparation of pseudocolored overlays of luminescence, fluorescence and grayscale images. We carried out fluorescence and luminescence imaging of tissues following sacrifice and dissection as described for the live animal imaging, but with field of view adjusted for image acquisitions.

Histological analysis of infected and uninfected tissue

For histological analyses, we euthanized mice via carbon dioxide intoxication. We photographed the gross lesions of the mice with pyomyositis with a digital camera before and after removal of the skin. Then we carefully dissected the soft tissues of the *S. aureus*-infected (right) leg. For comparison with uninfected tissues, we also dissected the corresponding portion of the uninfected (left) leg. We then fixed all tissues in 10% neutral buffered formalin for 48 hours at room temperature. We gross-sectioned the fixed tissues and then routinely processed them in a series of alcohol and xylene baths, paraffin-

embedded them, and stained 4 μm sections with hematoxylin and eosin (HE), or Gram stain as previously described.[41] Slides were examined by a veterinary pathologist (D.K.M.) for histopathologic interpretation. We acquired high resolution digital images with a DP71 camera (Olympus) mounted on a BX51 microscope (Olympus) with MicroSuite Pathology Edition Software (Olympus).

Target-to-background ratio measurements

We used IVIS 4.2 software to measure fluorescence intensity within regions of interest of mouse images acquired 45 minutes following TT probe administration. The following three groups of mice were included in the analysis: uninfected mice, *S. aureus*-infected mice and MN-negative *S. aureus*-infected mice. We determined target-to-background ratios as follows: for infected animals, the fluorescence measured within an ROI placed over the probe-activation site of the infected leg was divided by fluorescence measured within an ROI placed over the contralateral, uninfected leg. For each uninfected mouse, we calculated the ratio of fluorescence within ROIs of uninfected versus contralateral, uninfected leg. We subtracted the tissue autofluorescence level (measured within each ROI in the background fluorescence image (taken prior to probe administration)) from each of the corresponding ROI fluorescence values measured at the 45 minute time point prior to the ratio calculations.

Magnetic resonance imaging of infected mice

We carried out magnetic resonance imaging (MRI) with a 4.7 Tesla Varian Unity/INOVA small-bore scanner with a 25 mm diameter transmit/receive coil. First, we anesthetized the mice with isoflurane (3% induction, 1.5% maintenance) and transferred them to the scanner. Following localizer scans, we acquired three sets of T2-weighted fast spin-echo scans (one each in axial, coronal, and sagittal orientations). Pulse sequence parameters were TR/TE = 2000/60 ms, echo train length = 8, slice thickness of 0.8 mm, and in-plane resolution of 0.16 mm over a 256 × 256 acquisition matrix with 6 signal averages for a scan time of about 8 minutes per orientation. Overall scan time was about 30 minutes for each mouse.

Blood counts

For blood collection, we anesthetized mice with ketamine/xylazine and collected at least 150 μl blood from each mouse via submandibular venous puncture into an EDTA tripotassium salt multivette (Multivette 600 K3E; Sarstedt). We measured complete blood counts (CBC) from undiluted blood samples within 30 minutes of collection using a Sysmex XT-200i Automated Hematology Analyzer (Sysmex America, Inc.).

Supplementary Material

Refer to Web version on PubMed Central for supplementary material.

Acknowledgments

Research reported in this publication was supported by the National Institute of Allergy and Infectious Diseases of the U.S. National Institutes of Health under Award Numbers AI083211 (A. Horswill) and R21AI101391 (J. McNamara). The content is solely the responsibility of the authors and does not necessarily represent the official views of the U. S. National Institutes of Health. F. Hernandez was supported by a postdoctoral fellowship from the

American Heart Association. The authors thank J. Kavanaugh for technical assistance with bacterial cultures and R. Schmidt and J. Widness for sharing a Sysmex XT-200i Automated Hematology Analyzer (Sysmex America Inc.).

References

1. Agarwal V, Chauhan S, Gupta, Pyomyositis RK. Neuroimaging Clin N Am. 2011; 21:975–983. x. [PubMed: 22032510]
2. Carek PJ, Dickerson LM, Sack JL. Diagnosis and management of osteomyelitis. Am Fam Physician. 2001; 63:2413–2420. [PubMed: 11430456]
3. Clerc O, Prod'hom G, Greub G, Zanetti G, Senn L. Adult native septic arthritis: a review of 10 years of experience and lessons for empirical antibiotic therapy. J Antimicrob Chemother. 2011; 66:1168–1173. [PubMed: 21393124]
4. Hatzenbuehler J, Pulling TJ. Diagnosis and management of osteomyelitis. Am Fam Physician. 2011; 84:1027–1033. [PubMed: 22046943]
5. Hope-Roberts M, Wainwright M, Horobin RW. Real-time imaging of bacteria in living mice using a fluorescent dye. Biotech Histochem. 2011; 86:104–107. [PubMed: 20608773]
6. Leevy WM, et al. Optical imaging of bacterial infection in living mice using a fluorescent near-infrared molecular probe. J Am Chem Soc. 2006; 128:16476–16477. [PubMed: 17177377]
7. Leevy WM, et al. Noninvasive optical imaging of staphylococcus aureus bacterial infection in living mice using a Bis-dipicolylamine-Zinc(II) affinity group conjugated to a near-infrared fluorophore. Bioconjug Chem. 2008; 19:686–692. [PubMed: 18260609]
8. Ning X, et al. Maltodextrin-based imaging probes detect bacteria in vivo with high sensitivity and specificity. Nat Mater. 2011; 10:602–607. [PubMed: 21765397]
9. Panizzi P, et al. In vivo detection of Staphylococcus aureus endocarditis by targeting pathogen-specific prothrombin activation. Nat Med. 2011; 17:1142–1146. [PubMed: 21857652]
10. White AG, et al. Optical imaging of bacterial infection in living mice using deep-red fluorescent squaraine rotaxane probes. Bioconjug Chem. 2010; 21:1297–1304. [PubMed: 20536173]
11. Kong Y, et al. Imaging tuberculosis with endogenous beta-lactamase reporter enzyme fluorescence in live mice. Proc Natl Acad Sci U S A. 2010; 107:12239–12244. [PubMed: 20566877]
12. Yang W. Nucleases: diversity of structure, function and mechanism. Q Rev Biophys. 2011; 44:1–93. [PubMed: 20854710]
13. Kelemen BR, et al. Hypersensitive substrate for ribonucleases. Nucleic Acids Res. 1999; 27:3696–3701. [PubMed: 10471739]
14. Elias DR, Thorek DL, Chen AK, Czupryna J, Tsourkas A. In vivo imaging of cancer biomarkers using activatable molecular probes. Cancer Biomark. 2008; 4:287–305. [PubMed: 19126958]
15. Hernandez FJ, et al. Degradation of nuclease-stabilized RNA oligonucleotides in Mycoplasma-contaminated cell culture media. Nucleic Acid Ther. 2012; 22:58–68. [PubMed: 22229275]
16. Arnone A, et al. The extracellular nuclease of Staphylococcus aureus: structures of the native enzyme and an enzyme-inhibitor complex at 4 A resolution. Proc Natl Acad Sci U S A. 1969; 64:420–427. [PubMed: 5261023]
17. Cuatrecasas P, Fuchs S, Anfinsen CB. Catalytic properties and specificity of the extracellular nuclease of Staphylococcus aureus. J Biol Chem. 1967; 242:1541–1547. [PubMed: 4290246]
18. Cunningham L, Catlin BW, Privatdegarilhe M. A Deoxyribonuclease of Micrococcus-Pyogenes. J Am Chem Soc. 1956; 78:4642–4645.
19. Boerlin P, Kuhnert P, Hussy D, Schaellibaum M. Methods for identification of Staphylococcus aureus isolates in cases of bovine mastitis. J Clin Microbiol. 2003; 41:767–771. [PubMed: 12574280]
20. Behlke MA. Chemical modification of siRNAs for in vivo use. Oligonucleotides. 2008; 18:305–319. [PubMed: 19025401]
21. Vester B, Wengel J. LNA (locked nucleic acid): high-affinity targeting of complementary RNA and DNA. Biochemistry. 2004; 43:13233–13241. [PubMed: 15491130]

22. Pochon F, Privat De Garilhe M. Structure of oligonucleotides liberated by the action of desoxyribonuclease on Staphylococcus pyogenes. Bull Soc Chim Biol (Paris). 1960; 42:795–815. [PubMed: 13736435]
23. Kiedrowski MR, et al. Nuclease modulates biofilm formation in community-associated methicillin-resistant Staphylococcus aureus. PLoS One. 2011; 6:e26714. [PubMed: 22096493]
24. Beenken KE, et al. Epistatic relationships between sarA and agr in Staphylococcus aureus biofilm formation. PLoS One. 2010; 5:e10790. [PubMed: 20520723]
25. Weissleder R, Ntziachristos V. Shedding light onto live molecular targets. Nat Med. 2003; 9:123–128. [PubMed: 12514725]
26. Contag CH, et al. Photonic detection of bacterial pathogens in living hosts. Mol Microbiol. 1995; 18:593–603. [PubMed: 8817482]
27. Francis KP, et al. Monitoring bioluminescent Staphylococcus aureus infections in living mice using a novel luxABCDE construct. Infect Immun. 2000; 68:3594–3600. [PubMed: 10816517]
28. Xiong YQ, et al. Real-time in vivo bioluminescent imaging for evaluating the efficacy of antibiotics in a rat Staphylococcus aureus endocarditis model. Antimicrob Agents Chemother. 2005; 49:380–387. [PubMed: 15616318]
29. Beenken KE, Spencer H, Griffin LM, Smeltzer MS. Impact of extracellular nuclease production on the biofilm phenotype of Staphylococcus aureus under in vitro and in vivo conditions. Infect Immun. 2012; 80:1634–1638. [PubMed: 22354028]
30. de Marie S. Difficult-to-treat infections. Intensive Care Med. 1990; 16 (Suppl 3):S239–242. [PubMed: 2289998]
31. Wu PI, Edelman ER. Structural biomechanics modulate intramuscular distribution of locally delivered drugs. J Biomech. 2008; 41:2884–2891. [PubMed: 18706562]
32. Ferreira BT, Benchetrit LC, De Castro AC, Batista TG, Barrucand L. Extracellular deoxyribonucleases of streptococci: a comparison of their occurrence and levels of production among beta-hemolytic strains of various serological groups. Zentralbl Bakteriol. 1992; 277:493–503. [PubMed: 1303692]
33. Ferrieri P, Gray ED, Wannamaker LW. Biochemical and immunological characterization of the extracellular nucleases of group B streptococci. J Exp Med. 1980; 151:56–68. [PubMed: 6985648]
34. Moon AF, et al. Structural insights into catalytic and substrate binding mechanisms of the strategic EndA nuclease from Streptococcus pneumoniae. Nucleic Acids Res. 2011; 39:2943–2953. [PubMed: 21113026]
35. Marshall MV, Draney D, Sevick-Muraca EM, Olive DM. Single-dose intravenous toxicity study of IRDye 800CW in Sprague-Dawley rats. Mol Imaging Biol. 2010; 12:583–594. [PubMed: 20376568]
36. Kobayashi H, Longmire MR, Ogawa M, Choyke PL. Rational chemical design of the next generation of molecular imaging probes based on physics and biology: mixing modalities, colors and signals. Chem Soc Rev. 2011; 40:4626–4648. [PubMed: 21607237]
37. Matsui A, et al. Real-time, near-infrared, fluorescence-guided identification of the ureters using methylene blue. Surgery. 2010; 148:78–86. [PubMed: 20117811]
38. Rasmussen JC, et al. Human Lymphatic Architecture and Dynamic Transport Imaged Using Near-infrared Fluorescence. Transl Oncol. 2010; 3:362–372. [PubMed: 21151475]
39. Sevick-Muraca EM. Translation of near-infrared fluorescence imaging technologies: emerging clinical applications. Annu Rev Med. 2012; 63:217–231. [PubMed: 22034868]
40. Novick RP. Genetic systems in staphylococci. Methods Enzymol. 1991; 204:587–636. [PubMed: 1658572]
41. Stoltz DA, et al. Cystic fibrosis pigs develop lung disease and exhibit defective bacterial eradication at birth. Sci Transl Med. 2010; 2:29ra31.

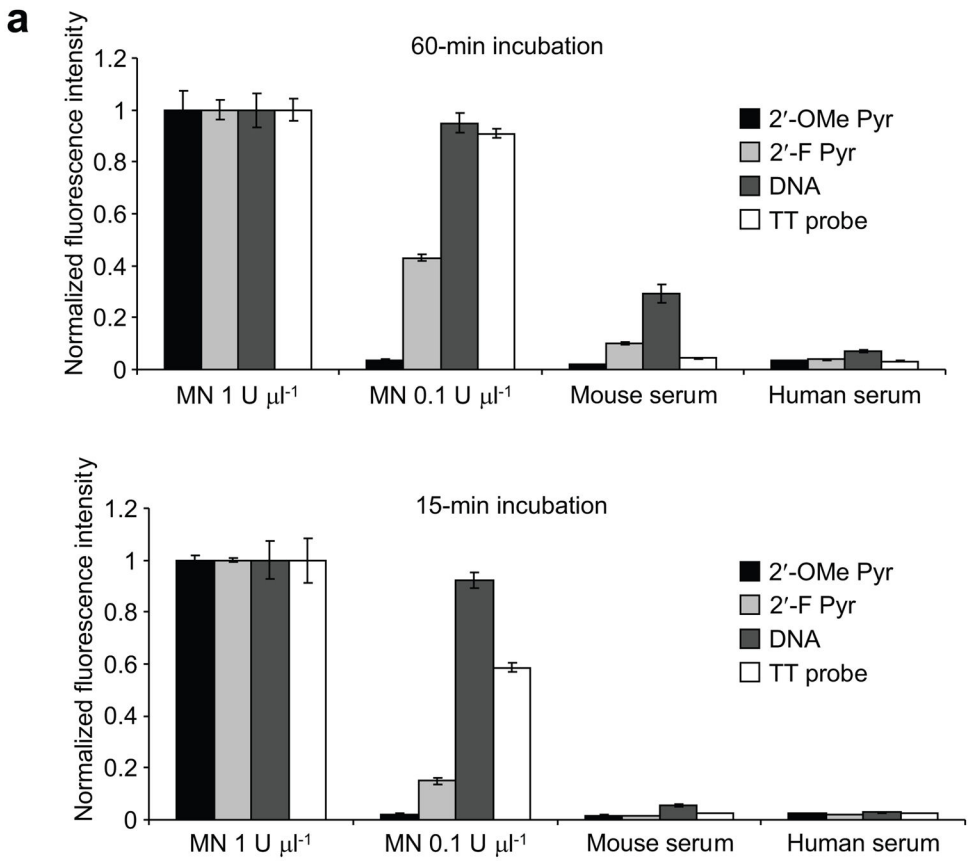

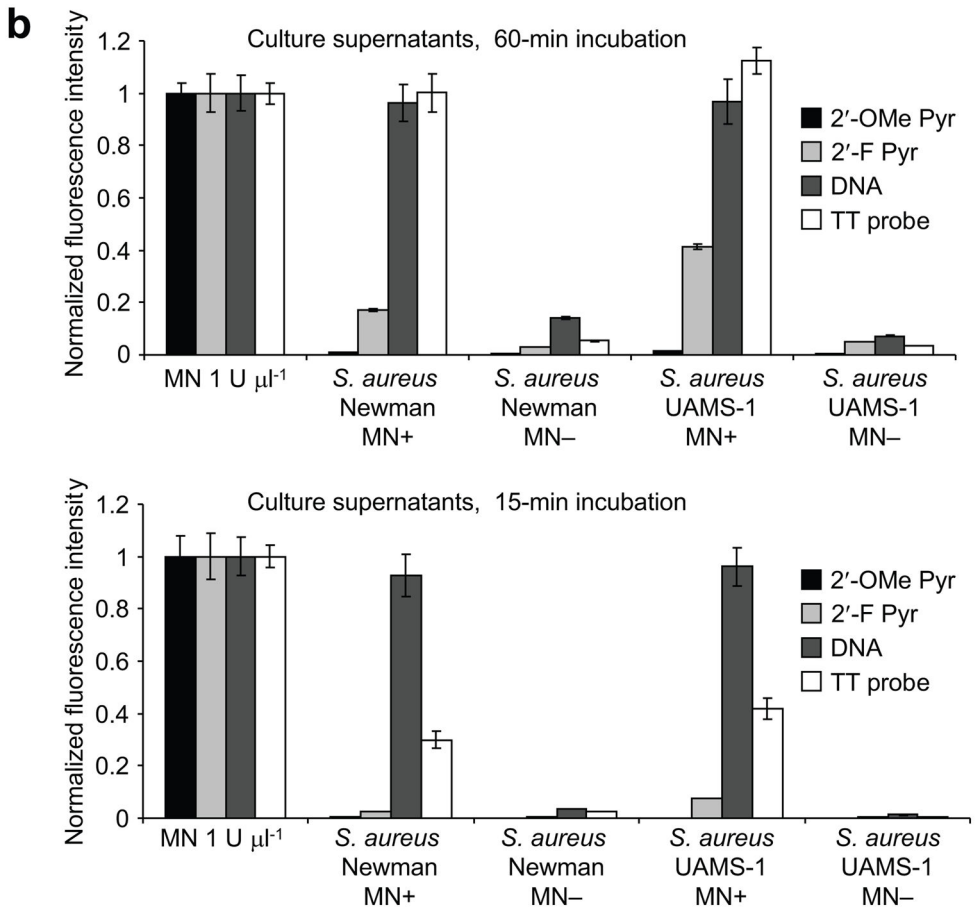

Figure 1.

Nucleic acid probe activation by MN and serum nucleases. Activation of various nucleic acid probes (see Table 1 for probe details) by MN, mouse and human serum (**a**), and *S. aureus* MN-expressing and MN-negative (Newman and UAMS-1 strains) culture supernatants (**b**). Each of the indicated probes was incubated at 37 °C with 1 U μl^{-1} (positive control) or 0.1 U μl^{-1} MN in DPBS (includes physiological levels of calcium and magnesium), or with 90% mouse or human serum (**a**) or with 90% of culture supernatants of the indicated *S. aureus* strains (prepared as described in **Methods**). Mean fluorescence values of all reactions (measured in triplicate) with a given probe were normalized to the mean fluorescence measured with digestion of the probe with 1 U μl^{-1} MN. Error bars represent standard deviations of the triplicate fluorescence measurements. Background fluorescence subtractions were carried out (prior to normalization) as follows: The fluorescence of each of the probes incubated in DPBS was subtracted from the corresponding MN-containing reactions. The fluorescence of each of the probes incubated in DPBS plus the autofluorescence of each serum (mouse or human) was subtracted from the serum-containing reactions. The fluorescence of each of the probes incubated in unconditioned TSB was subtracted from the corresponding *S. aureus* culture supernatant reactions.

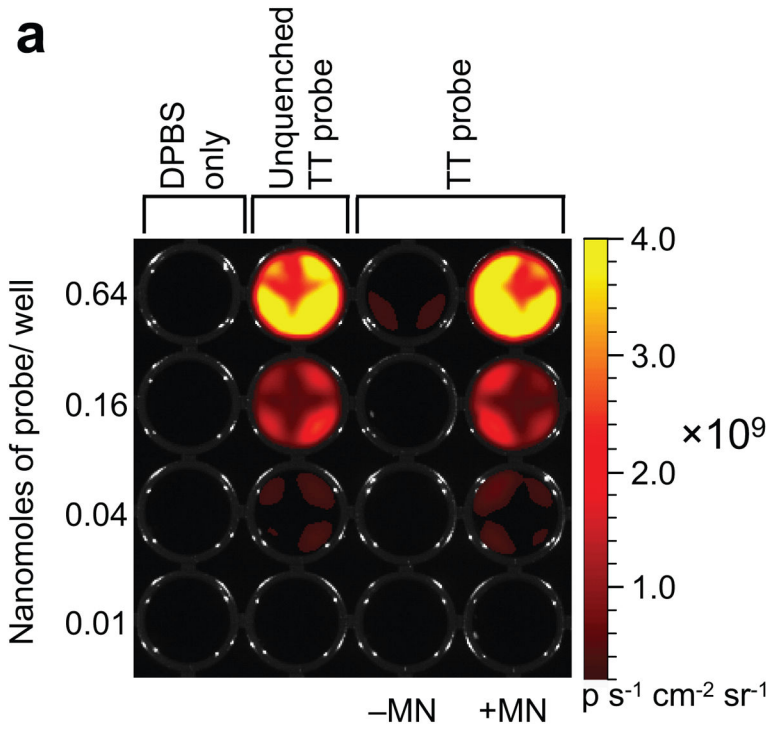

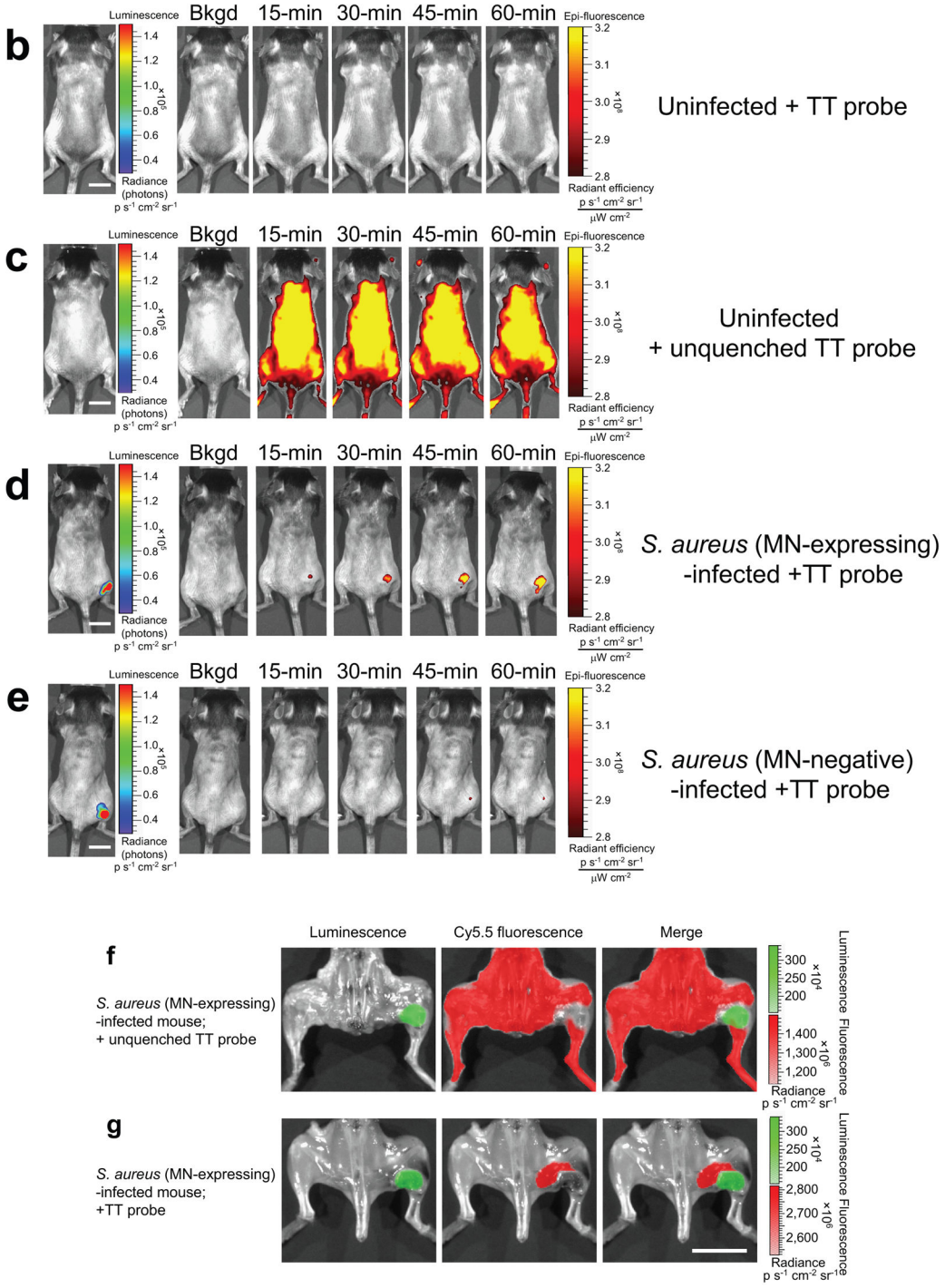

Figure 2.

Activation of the Cy5.5-TT probe by MN *in vitro* and in *S. aureus*-infected mice. For *in vitro* evaluation (**a**), the indicated amounts of probe were incubated with (+MN) or without (−MN) MN at 37 °C for 1 hour. Controls include buffer only (DPBS) and the unquenched TT probe. To evaluate probe activation in mice with *S. aureus*-derived pyomyositis, uninfected mice (**b**, n = 4 mice; **c**, n = 3 mice), and mice infected with *lux*+ MN-expressing

S. aureus (**d**, n = 5 mice), or with *lux*+ MN-negative *S. aureus* (**e**, n = 4 mice) in the right thighs were imaged with Cy5.5-channel fluorescence prior to (Bkgd) and after tail vein administration of Cy5.5-TT probe (**b**, **d**, **e**) or unquenched TT probe (**c**). Luminescence images acquired prior to probe injections (panels on left) indicate location of infections (in **d** and **e**). Lookup tables indicate the relationship between pseudocolors and signal strength. Fluorescence display levels are adjusted to show light levels that exceed tissue autofluorescence, unactivated TT probe fluorescence and the low levels of luminescent light bleed-through and activation by serum nucleases. Times listed above fluorescence images indicate the time elapsed after probe administration. For post-sacrifice and dissection imaging, mice with thigh-muscle *lux*+, MN-expressing *S. aureus* pyomyositis, injected with unquenched TT probe (**f,** n = 4 mice) or TT probe (**g,** n = 4 mice) were sacrificed 45 minutes after probe injection; dissected muscle tissue was imaged with luminescence and the Cy5.5 fluorescence channel. Scale bars = 1 cm.

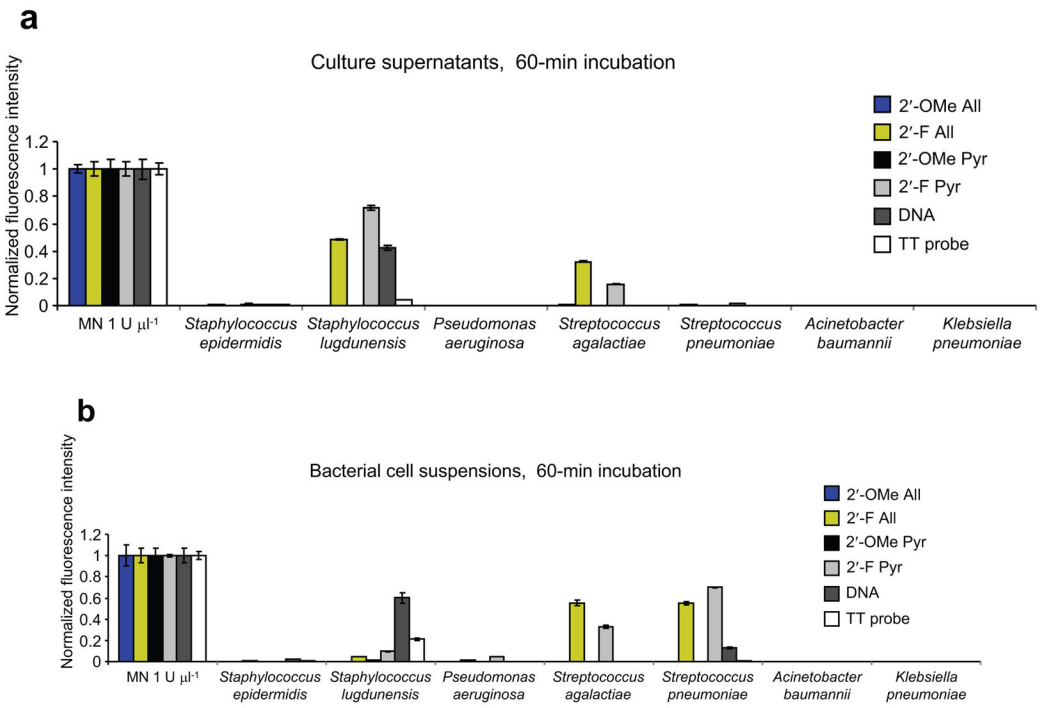

Figure 3.

Nucleic acid probe activation in cultures of additional bacterial pathogens. Activation of various nucleic acid probes (see Table 1 for probe details) by culture supernatants (**a**) or cell suspensions (**b**) of various pathogenic bacterial species. Each of the indicated probes was incubated with 1 U μl^{-1} MN (positive control) in DPBS or with 90% of culture supernatants or concentrated and washed cell suspensions of the indicated bacterial species (prepared as described in **Methods**) at 37 °C. Mean fluorescence values of all reactions (measured in triplicate) with a given probe were normalized to the mean fluorescence measured with digestion of the probe with 1 U μl^{-1} MN. Error bars represent standard deviations of the triplicate fluorescence measurements. Background fluorescence subtractions were carried out (prior to normalization) as follows: The fluorescence of each of the probes incubated in DPBS was subtracted from the corresponding MN-containing reactions. The fluorescence of each of the probes incubated in the appropriate unconditioned culture broth was subtracted from the corresponding culture supernatant reactions. The fluorescence of each of the probes incubated in DPBS plus the autofluorescence of each appropriate bacterial suspension was subtracted from each bacterial suspension reaction. The data shown were collected in several distinct experiments, each of which included the above-mentioned positive controls (for normalization) and background measurements (for subtractions).

Table 1

Nuclease probe sequences and modifications.

2′-F Pyr	FAM–	fU	fC	fU	fC	rG	fU	rA	fC	rG	fU	fU	fC	–ZEN–RQ
2′-OMe Pyr	FAM–	mU	mC	mU	mC	rG	mU	rA	mC	rG	mU	mU	mC	–ZEN–RQ
2′-F All	FAM–	fU	fC	fU	fC	fG	fU	fA	fC	fG	fU	fU	fC	–ZEN–RQ
2′-OMe All	FAM–	mU	mC	mU	mC	mG	mU	mA	mC	mG	mU	mU	mC	–ZEN–RQ
DNA	FAM–	**T**	**T**	**C**	**C**	**T**	**T**	**C**	**C**	**T**	**C**	–ZEN–RQ		
AT probe	FAM–	mC	mU	mC	mG	**A**	**T**	mC	mG	mU	mU	mC	–ZEN–RQ	
AA probe	FAM–	mC	mU	mC	mG	**A**	**A**	mC	mG	mU	mU	mC	–ZEN–RQ	
TT probe (FAM-labeled)	FAM–	mC	mU	mC	mG	**T**	**T**	mC	mG	mU	mU	mC	–ZEN–RQ	
TT probe (Cy5.5-labeled)	Cy5.5–	mC	mU	mC	mG	**T**	**T**	mC	mG	mU	mU	mC	–ZEN–RQ	
Unquenched TT probe	Cy5.5–	mC	mU	mC	mG	**T**	**T**	mC	mG	mU	mU	mC	–InvdT	

FAM = FAM fluorophore (fluorescein amidite); ZEN =IDT “ZEN” fluorescence quencher; RQ = IDT Iowa Black® RQ fluorescence quencher; mA = 2′-*O*-methyl-Adenosine; mC = 2′-*O*-methyl-Cytidine; mG = 2′-*O*-methyl-Guanosine; mU = 2′-*O*-methy-Uridine; fA = 2′-fluoro-Adenosine; fC = 2′-fluoro-Cytidine; fG = 2′-fluoro-Guanosine; fU = 2′-fluoro-Uridine; Nucleotides written in **bold** are deoxy nucleotides (DNA); InvdT = inverted dT.